Received: 13 May 2022 | Revised: 12 July 2022 | Accepted: 25 July 2022

DOI: 10.1111/cas.15516

ORIGINAL ARTICLE

Cancer Science WILEY

Nonhematogenic circulating aneuploid cells confer inferior prognosis and therapeutic resistance in gliomas

Mingxiao Li[1,2] | Faliang Gao[3,4] | Xiaohui Ren[1,2] | Gehong Dong[5] | Hongyan Chen[6] | Alexander Y. Lin[7] | Daisy Dandan Wang[7] | Mingyang Liu[8] | Peter Ping Lin[7] | Shaoping Shen[1,2] | Haihui Jiang[1,2] | Chuanwei Yang[1,2] | Xiaokang Zhang[1,2] | Xuzhe Zhao[1,2] | Qinghui Zhu[1,2] | Ming Li[1,2] | Yong Cui[1,2] | Song Lin[1,2,9,10]

[1]Department of Neuro-Surgical Oncology, National Clinical Research Center for Neurological Diseases, Capital Medical University, Beijing, China

[2]Department of Neurosurgery, Beijing Neurosurgical Institute, Capital Medical University, Beijing, China

[3]Department of Neurosurgery, Zhejiang Provincial People's Hospital, People's Hospital of Hangzhou, People's Hospital of Hangzhou Medical College, Hangzhou, Zhejiang, China

[4]Key Laboratory of Endocrine Gland Diseases of Zhejiang Province, Hangzhou, Zhejiang, China

[5]Department of Pathology, Beijing Tiantan Hospital, Capital Medical University, Beijing, China

[6]Department of Radiology, Beijing Tiantan Hospital, Capital Medical University, Beijing, China

[7]Cytelligen, San Diego, California, USA

[8]Department of Medicine, University of Oklahoma Health Science Center, Oklahoma City, Oklahoma, USA

[9]Center of Brain Tumor, Beijing Institute for Brain Disorders, Beijing, China

[10]Beijing Key Laboratory of Brain Tumor, Beijing, China

Correspondence
Yong Cui, Department of Neurosurgical Oncology, Beijing Tiantan Hospital, Beijing Neurosurgical Institute, Capital Medical University, Beijing 100070, China.
Email: cuiyong20130422@163.com

Song Lin, Department of Neurosurgical Oncology, Beijing Tiantan Hospital, Capital Medical University, Center of Brain Tumor, Beijing Institute for Brain Disorders, Beijing Key Laboratory of Brain Tumor, China National Clinical Research Center for Neurological Diseases, Beijing 100070, China.
Email: linsong2005@126.com

Funding information
Capitals Funds for Health Improvement and Research, Grant/Award Number: 2020-2-1075; National Natural Science Foundation of China, Grant/Award Number: 81771309

Abstract

Aneuploidy is the hallmark of malignancy. Our previous study successfully detected nonhematogenic circulating aneuploidy cells (CACs) in types of gliomas. The current prospective clinical study aims to further precisely subcategorize aneuploid CACs, including $CD31^-$ circulating tumor cells (CTCs) and $CD31^+$ circulating tumor endothelial cells, and thoroughly investigate the clinical utilities of these different subtypes of cells. Co-detection and analysis of CTCs and circulating tumor-derived endothelial cells (CTECs) expressing CD133, glial fibrillary acidic protein (GFAP), or epidermal growth factor receptor variant III (EGFR vIII) were performed by integrated subtraction enrichment and immunostaining fluorescence in situ hybridization (SE-iFISH) in 111 preoperative primary diffuse glioma patients. Aneuploid CACs could be detected in most de novo glioma patients. Among detected CACs, 45.6% were $CD31^-/CD45^-$ aneuploid CTCs and the remaining 54.4% were $CD31^+/CD45^-$ aneuploid CTECs. Positive detection of CTECs significantly correlated with disruption of the blood–brain barrier. The median number of large CTCs ($_L$CTCs, >5 μm, 2) in

Abbreviations: BBB, blood–brain barrier; CAC, circulating aneuploid cells; CTC, circulating tumor cells; CTEC, circulating tumor-derived endothelial cells; CTSC, circulating tumor stem cell; GBM, glioblastoma; HGA, high-grade astrocytoma; HGG, high-grade glioma; LGA, low-grade astrocytoma; LGG, low-grade glioma; SE-iFISH, subtraction enrichment integrated with immunostaining fluorescence in situ hybridization; VM, vasculogenic mimicry.

low-grade glioma (WHO grade 2) was less than high-grade glioma (WHO grades 3 and 4) (3, $p = 0.044$), but this difference was not observed in small CTCs ($_S$CTCs, ≤5 μm), CTECs or CACs (CTCs + CTECs). The numbers of CTCs, CTECs, or CACs in patients with contrast-enhancing (CE) lesions considerably exceeded that of non-CE lesions ($p < 0.05$). Receiver operating characteristic curves demonstrated that CD31$^+$ CTECs, especially $_L$CTECs, exhibited a close positive relationship with CE lesions. Survival analysis revealed that the high number of CD31$^-$ CTCs could be an adverse factor for compromised progression-free survival and overall survival. Longitudinal surveillance of CD31$^-$ CTCs was suitable for evaluating the therapeutic response and for monitoring potential emerging treatment resistance.

KEYWORDS
blood–brain-barrier, CD31-CTC, CD31 + CTEC, glioma, prognosis, therapy resistance

1 | INTRODUCTION

Gliomas, the most common de novo brain tumor in adults, tend to exhibit a bleak outcome.[1] Maximal safe surgical removal of tumors with or without subsequent chemoradiotherapy constitutes the mainstay of alleviating symptoms and prolonging survival. Nevertheless, the complete cellular removal of diffuse gliomas is impossible, due to intrinsically aggressive tumor behavior, the infiltrative pattern of tumor growth, and the ambiguous border present in normal brain tissue.[2] Therefore, inevitable postsurgical tumor recurrence is the most prominent problem of gliomas.

Patterns of glioma progression predominately present local recurrence, which means that tumor cells regrow in the vicinity of the primary resection cavity.[3] However, ~20% of patients displayed novel lesions located far from the initial tumor bed or even in extracranial viscera, including liver, lung, vertebra, and so forth, implying a subgroup of glioma cells immigrated to a distant but suitable milieu where metastatic tumor cells could reproduce unlimitlessly.[4,5] Such an occurrence overturns the traditional theory that glioma cells do not penetrate the BBB composed of CD31$^+$ brain microvascular endothelial cells (BMECs)[6] and propagate out of the central nervous system. The concept of CTCs provided a rational explanation in terms of glioma intracranial dissemination and extracranial metastasis. However, compared with visceral epithelial solid tumor CTCs, the unavailable expression of ubiquitous surface markers on glioma cells has resulted in most conventional CTC technologies being unsuitable for glioma CTC detection.[7–9] Although the use of combined multimarkers to investigate the clinical significance of glioma CTCs in patients with advanced GBM has been reported,[10–12] great efforts are required to further improve relevant strategies.[13]

Aneuploidy, referring to aberrant gain or loss of chromosomes in a cell, is the hallmark of tumor cells. Aneuploidy plays a critical role in cancer cell malignancy, therapeutic resistance, cancer metastasis, and tumor recurrence.[14–17] Previously, we successfully detected nonhematogenic aneuploid CACs in seven diverse subtypes of brain glioma and reported their significance.[18] In the present study, the impact and clinical significance of aneuploid CD31$^-$ CTCs and CD31$^+$ CTECs on glioma patient BBB disruption,[17,19] chemoradiotherapeutic efficacy, tumor progression, and recurrence were comprehensively investigated.

2 | MATERIALS AND METHODS

2.1 | Patients

In total, 111 newly diagnosed adult patients with diffuse glioma (WHO grades 2–4), including 67 men and 44 women with a mean age of 44.8 ± 12.4 years old, were prospectively enrolled from November 2017 to November 2018 (Table 1). All the enrolled patients were subjected to surgical resection, followed by receiving chemoradiotherapy or just observation that conformed to the latest National Comprehensive Cancer Network (NCCN) guidelines. Follow-up was regularly performed every 1 month or 3 months regarding the patients' situations. Progression-free survival was defined as the duration from the initial surgery to the time of tumor progression and overall survival (OS) was defined as the duration between the initial surgery and the patient's death, or last follow-up.[20,21]

Signed consent forms were received from every patient. The study was approved by the institutional review board of the Capital Medical University and performed according to the Declaration of Helsinki Principles.

2.2 | SE-iFISH

SE-iFISH was performed according to the manufacture's instructions (Cytelligen, San Diego, CA, USA).[19] Briefly, 6 ml of peripheral blood (PB) in fasting patients were collected into an acid citrate dextrose (ACD) anticoagulant tube (Becton Dickinson), followed by centrifugation at 600 *g* for 5 min. Sedimented blood cells

TABLE 1 Quantitative analysis of aneuploid CTCs and CTECs in patients with different types of gliomas

			Aneuploid CTCs (median)				Aneuploid CTECs (median)			
Pathology	Grade	*n*	Monoploid	Triploid	Multiploid	Total	Monoploid	Triploid	Multiploid	Total
A-m	2	25	0	2.0	1.0	4.0	0	1.0	5.0	7.0
A-w	2	6	0	0.0	3.5	3.5	0	0.5	12.5	9.0
O	2	18	0	2.0	3.0	4.5	0	0.5	5.0	10
A-m	3	5	4.0	4.0	2.0	4.0	0	0	5.0	6.0
A-w	3	8	0	3.0	10.0	13.0	0	1.0	13.5	15.0
O	3	6	0	1.5	1.5	2.0	0	1.5	5.5	8.0
A-m	4	6	0	4.0	4.0	6.5	0	3.5	9.0	11.5
GBM-w	4	37	0	3.0	3.0	6.0	0	0.0	6.0	7.0

Abbreviations: A-m, astrocytoma, IDH mutant; A-w, astrocytoma, IDH-wildtype; GBM-w, glioblastoma, IDH-wildtype, WHO grade 4; O, oligodendroglioma, IDH mutant and 1p/19q co-deleted.

loaded on the top of 3.5 ml of nonhematologic cell separation matrix were spun at 400 *g* for 5 min. The solution containing white blood cells (WBCs) and tumor cells was subsequently incubated with 150 μl of immunomagnetic beads conjugated to a mixture of anti-leukocyte mAbs for 15 min. WBCs bound to immunobeads were depleted using a 50-ml size magnetic separator (Cytelligen). The magnetic beads-free solution was collected and mixed with human CTC buffer to 14 ml. Samples were centrifuged at 400 *g* for 5 min. Sedimented cells were resuspended and mixed with the cell fixative, and subsequently coated on CTC slides. Dried cells were ready for iFISH processing.

Five-color iFISH was performed according to the manufacture's updated protocol (Cytelligen). Briefly, dried monolayer cells on the coated slides were hybridized with the Vysis chromosome 8 centromere probe (CEP8) SpectrumOrange (Abbott Laboratories) for 4 h using a S500 StatSpin ThermoBrite Slide Hybridization/Denaturation System (Abbott Molecular). Samples were subsequently incubated with the indicated fluorescence labeled monoclonal antibodies (Cytelligen), including Alexa Fluor (AF)594-anti-CD45 (Clone 9.4), AF488-anti-CD133 (Clone AC133), and Cy5-anti-CD31(Clone WM59) at room temperature for 20 min in the dark. After washing, samples were mounted with 4′,6-diamidino-2-phenylindole (DAPI) mounting medium (Vector Laboratories), and subsequently subjected to the Metafer-i•FISH® CTC 3D scanning and image analyzing system co-developed by Carl Zeiss, MetaSystems, and Cytelligen.[19] Identification criteria of a positive cell: CTC, $DAPI^+/CD45^-/CD31^-$/aneuploid CEP8; CTSC, $DAPI^+/CD45^-/CD31^-/CD133^+$/aneuploid CEP8; CTEC, $DAPI^+/CD45^-/CD31^+$/aneuploid CEP8.

2.3 | Histopathological and molecular diagnosis

The IDH1 R132/IDH2 R172, TERT promoter (C228T/C250T) mutation was tested by next generation sequencing and the status of 1p/19q, +7/10−, EGFR amplification was determined using fluorescence in situ hybridization (FISH).[22,23]

2.4 | Collection of radiological data

All patients underwent a conventional plain scan and a contrast-enhancing (CE) T1-weighted scan using a 3.0T magnetic resonance imaging (MRI) scanner, including axial plain T1, T2, FLAIR images, as well as axial, sagittal, and coronary contrast-enhanced T1 images.[24] A crossing review of MR images was performed by two experienced radiologists to define the modes of recurrence.

2.5 | Statistical analysis

Student's *t*-test was applied for analysis of continuous variables, and the Mann–Whitney *U*-test was applied for nonparametric data. Chi-squared test or Fisher's exact test was applied to compare the categorical variables. Survival as a function of time was plotted using the Kaplan–Meier method and compared using log-rank analysis. SPSS version 25.0 (IBM Corporation) and GraphPad Prism 8.0.1 (GraphPad Software) were applied for statistical analysis. Probability values were obtained using two-sided tests. Values of $^*p < 0.05$ and $^{**}p < 0.01$ were considered statistically significant and very significant, respectively.

3 | RESULTS

3.1 | Analysis of aneuploid CTCs and CTECs co-detected in glioma patients

Revealed in Figure 1A, iFISH was applied to perform in situ phenotypic and karyotypic characterization of glioma aneuploid $CD31^-$ CTCs and $CD31^+$ CTECs. A large (>5 μm WBC) multiploid (≥tetrasomy 8) CTC ($_L CTEC^{multi}$) and a small (≤5 μm) triploid CTC ($_S CTC^{tri}$) are shown in Figure 1Aa/b, respectively. A multiploid CTEC in large cell size ($_L CTEC^{multi}$) and a small multiploid CTEC ($_S CTEC^{multi}$) are revealed in Figure 1Ac/d, respectively. Figure 1Ae showed a stemness marker $CD133^+$ large multiploid CTSC ($_L CTSC^{multi}$), which was detected in five out of 34 examined

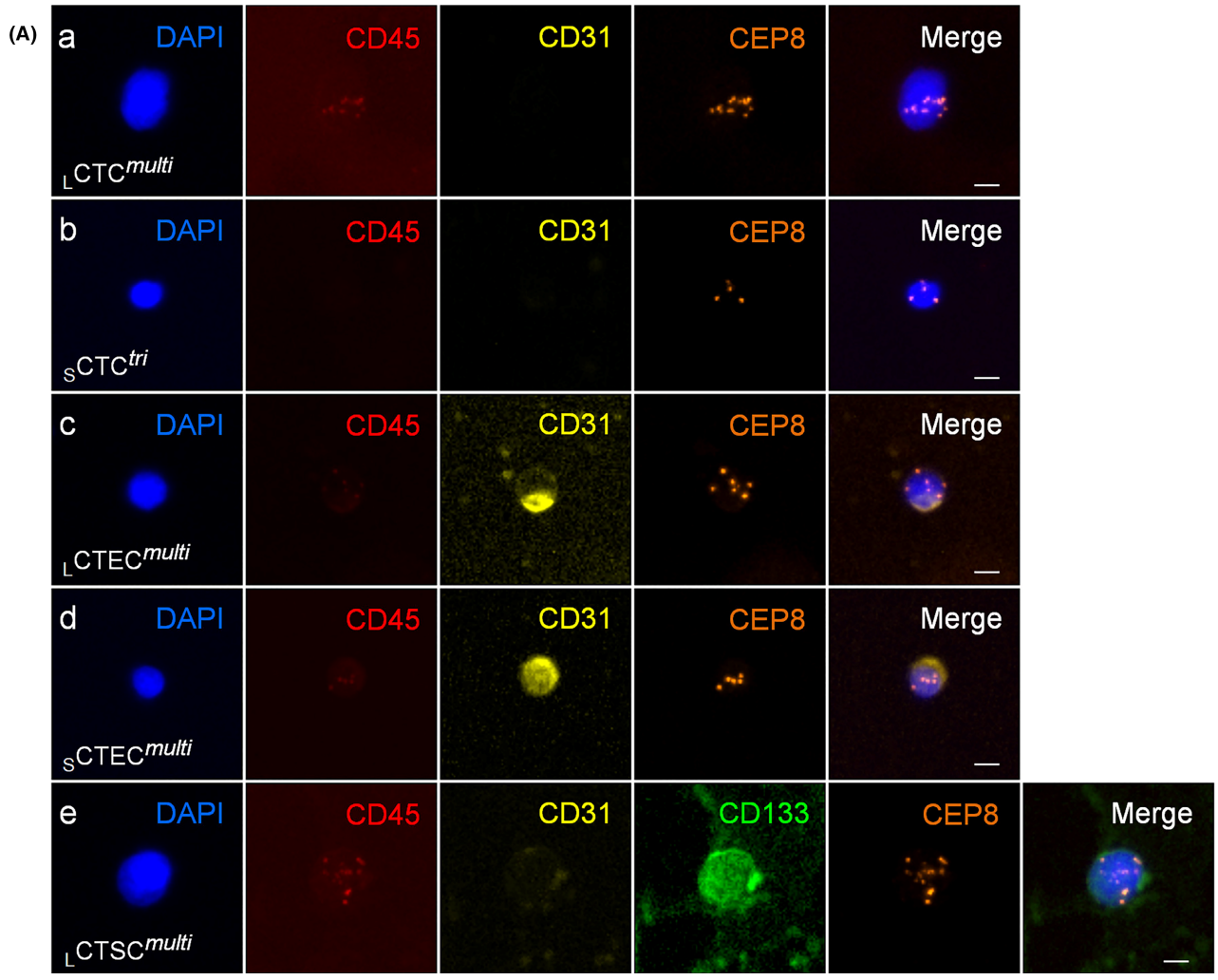
(A)
a DAPI CD45 CD31 CEP8 Merge
LCTCmulti
b DAPI CD45 CD31 CEP8 Merge
SCTCtri
c DAPI CD45 CD31 CEP8 Merge
LCTECmulti
d DAPI CD45 CD31 CEP8 Merge
SCTECmulti
e DAPI CD45 CD31 CD133 CEP8 Merge
LCTSCmulti

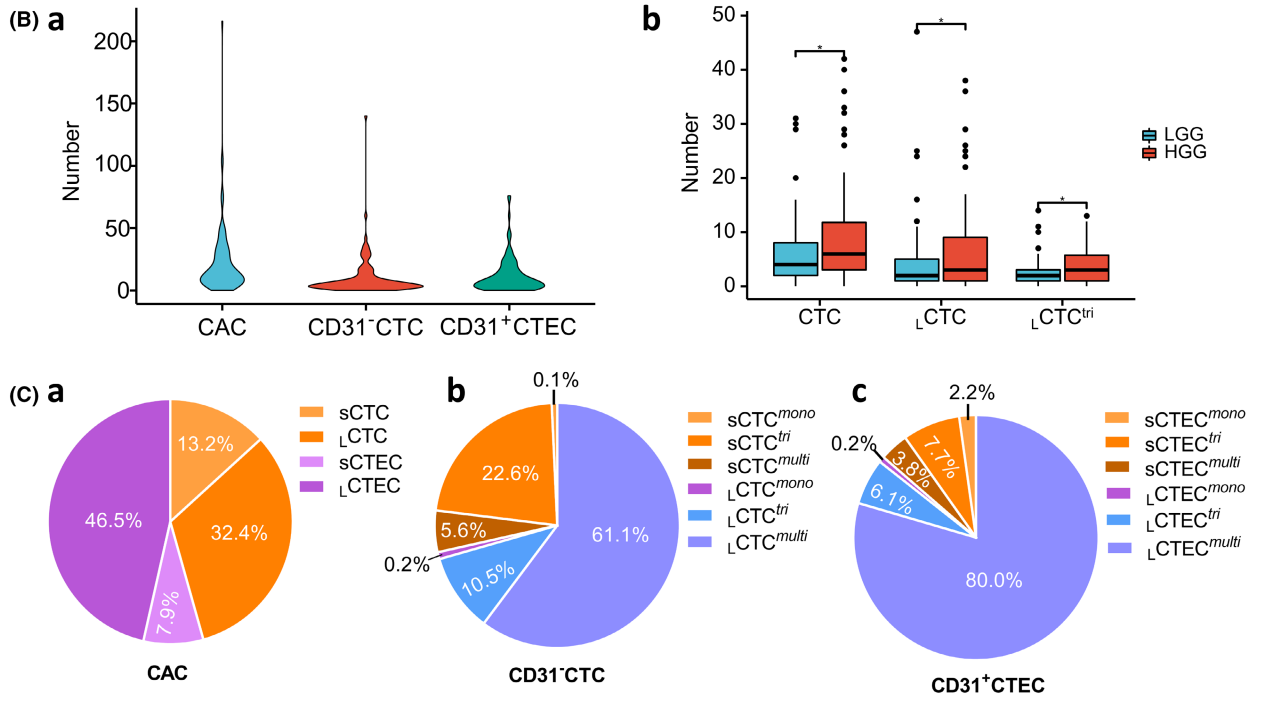
(B) a
Number
200
150
100
50
0
CAC
CD31-CTC
CD31+CTEC
b
Number
50
40
30
20
10
0
CTC
LCTC
LCTCtri
LGG
HGG
(C) a
13.2%
32.4%
7.9%
46.5%
sCTC
LCTC
sCTEC
LCTEC
CAC
b
0.1%
22.6%
5.6%
0.2%
10.5%
61.1%
sCTCmono
sCTCtri
sCTCmulti
LCTCmono
LCTCtri
LCTCmulti
CD31-CTC
c
2.2%
0.2%
7.7%
3.8%
6.1%
80.0%
sCTECmono
sCTECtri
sCTECmulti
LCTECmono
LCTECtri
LCTECmulti
CD31+CTEC

FIGURE 1 The iFISH images of glioma aneuploid CTCs and CTECs. (A-a) A large cell-sized (>5 μm) multiploid (≥tetrasomy 8) CTC ($_{L}CTC^{multi}$). (A-b) A triploid small (≤5 μm) CTC ($_{S}CTC^{tri}$). (A-c) A large multiploid CTEC ($_{L}CTEC^{multi}$). (A-d) A small multiploid CTEC ($_{S}CTEC^{multi}$). (A-e) A large multiploid CD133^{+} CTSC ($_{L}CTSC^{multi}$). Bars, 5 μm. (B) Quantification of CTCs, CTECs, and CACs (CTCs + CTECs). (B-a) Overall analysis: 1105 total CD31^{-} CTCs with a median of five cells, 1316 total CD31^{+} CTECs with a median of seven cells, and 2421 total CACs with a median of 13 cells. (B-b) Comparison of CTCs and their subtypes in 49 LGG and 62 HGG patients. Medians of cell numbers are 4.0 (0–61, LGG, red) versus 6.0 (0–140, HGG, blue) for overall CTCs ($p = 0.050$), 2.0 (0–47, LGG) versus 3.0 (0–138, HGG) for $_{L}CTCs$ ($^{*}p = 0.044$), and 0 (0–14, LGG) versus 1 (0–13, HGG) for $_{L}CTCs^{tri}$ ($^{*}p = 0.032$) (Mann–Whitney *U*-test). (C) Composition analysis. (C-a) CACs consist of 45.6% CTCs (including 32.4% large and 13.2% small cells), and 54.4% CTECs (46.5% large and 7.9% small cells). (C-b) CTCs are mainly composed of large multiploid ($_{L}CTCs^{multi}$, 61.1%) and small triploid ($_{S}CTCs^{tri}$, 22.6%) cells. (C-c) The majority of CTECs (80%) is large multiploid cells ($_{L}CTECs^{multi}$).

patients (5/34, 14.7%), including three GBM, two astrocytomas (IDH mutant and 1p/19q intact, WHO grade 3), and one oligodendroglioma (IDH mutant and 1p/19q co-deleted, WHO grade 3) subjects. For patients with GBM, CD133^{+} CTCs were detected in 30% GBM patients (3/10), which surpassed EGFR vIII^{+} CTC (14.8%, 4/27) and GFAP^{+} CTC (0%, 0/27).

Figure 1Ba demonstrates an overview of the detected 1105 aneuploid CTCs, 1316 CTECs, and 2421 CACs (CTCs + CTECs) with a median of five cells (0–140) for CTCs, 7 (0–140) for CTECs, and 13 (0–216) for CACs. As depicted in Figure 1Bb, the quantities of CTCs and their subtypes in HGGs (WHO grades 3 and 4; Table 1) were higher than the malignant LGGs (WHO grade 2; Table 1), showing medians of cell numbers of 4.0 (0–61, $n = 49$ LGG) versus 6.0 (0–140, $n = 62$ HGG) for overall CTCs ($p = 0.050$), 2.0 (0–47, LGG) versus 3.0 (0–138, HGG) for $_{L}CTCs$ ($^{*}p = 0.044$), and 0 (0–14, LGG) versus 1 (0–13, HGG) for $_{L}CTCs^{tri}$ ($^{*}p = 0.032$) (Mann–Whitney *U*-test). Additional comparisons performed on following cohorts did not show statistically significant differences: IDH1/2 mutant astrocytoma (grade 2, $n = 25$) versus IDH1/2 mutant high-grade astrocytoma (grade 3, $n = 11$) ($p = 0.103$); oligodendroglioma (grade 2, $n = 18$) versus oligodendroglioma (grade 3, $n = 6$) ($p = 0.986$); and IDH 1/2 wild-type astrocytoma (histological grade 2, $n = 6$) versus IDH 1/2 wild-type high-grade astrocytoma (histological grades 3 and 4, $n = 45$) ($p = 0.196$). In addition, no significant difference was observed among diverse subtypes of CTECs between LGG and HGG cohorts.

Dissected compositions of CTCs, CTEC,s and CACs are shown in Figure 1C. As demonstrated in Figure 1Ca, CTCs and CTECs in overall CACs were 45.6% and 54.4%, respectively. The majority of each category of cells was large cells, revealing 32.4% out of 45.6% for $_{L}CTCs$ and 46.5% out of 54.4% for $_{L}CTECs$. For the remaining small cells, the percentage of $_{S}CTCs$ (13.2%) was higher than 7.9% of $_{S}CTECs$, indicating that CTCs had more small cells. Comprehensive morphological and karyotypic analysis indicated that the main populations of CTCs were composed of large multiploid ($_{L}CTCs^{multi}$, 61.1%) and small triploid ($_{S}CTCs^{tri}$, 22.6%) cells (Figure 1Cb), whereas 80% of CTECs were large multiploid cells ($_{L}CTECs^{multi}$), as revealed in Figure 1Cc.

3.2 | Quantity of large cell-sized multiploid CTECs ($_{L}CTECs^{multi}$) increased in patients with CE lesions

Unlike MRI non-CE lesions revealed in Figure 2Aa,b, MRI CE lesions in patients are an evident sign of BBB damage and malformed neovascularization (red arrows in Figure 2Ac/d). Quantitative analysis of CD31^{-} CTCs and CD31^{+} CTECs in CE ($n = 81$) and non-CE subjects ($n = 30$) is depicted in Figure 2Ba–c. As demonstrated in Figure 2Ba, the medians of cell numbers in the CE lesion cohort (red bar) increased in comparison with non-CE lesion patients (blue bar), showing media of 6.0 (0–140, CE) versus 3.0 (1–31, non-CE) for CTCs ($^{*}p = 0.023$, Mann–Whitney *U*-test), 9.0 (0–76, CE) versus 5.0 (0–33, non-CE) for CTECs ($^{**}p = 0.006$), and 15.0 (1–216, CE) versus 8.5 (1–49, non-CE) for CACs ($^{**}p = 0.007$). Revealed in Figure 2Bb, further morphological analysis indicated that only $_{L}CTCs$ and $_{L}CTECs$ accounted for the increased cell numbers in CE patients ($_{L}CTCs$: CE, median 3.0, 0–138, non-CE, median 1.0, 0–25, $^{**}p = 0.009$; $_{L}CTECs$: CE, median 7.0, 0–75, non-CE: median 3.0 0–29, $^{**}p = 0.002$), whereas both $_{S}CTCs$ and $_{S}CTECs$ did not show significant differences. Depicted in Figure 2Bc, additional karyotypic analysis demonstrated that between those increased $_{L}CTCs$ and $_{L}CTECs$, the particular subtype of $_{L}CTECs^{multi}$ harbored the most marked difference, between CE (median 7.0, 0–75) and non-CE lesion (median 3.0, 0–28) cohorts ($^{**}p = 0.002$), compared with $_{L}CTCs^{multi}$ showing 2.0 (0–134, CE) versus 1.0 (0–12, non-CE), $^{*}p = 0.024$.

Area under the ROC curve (AUC)–ROC analysis was performed to dissect the correlation between cell numbers and MRI contrast (Figure 2C). Figure 2Ca shows AUC values of AUC_{CTEC} (**0.670) > AUC_{CAC} (**0.665) > AUC_{CTC} (*0.640). Stratification analysis indicated that beyond $_{L}CTECs$ (**0.692, Figure 2Cb) and $_{L}CTCs$ (**0.660), $_{L}CTECs^{multi}$ (**0.690, Figure 2Cc), rather than $_{L}CTCs^{multi}$ (*0.638), was the most significant biomarker relevant to distorted neovascularization and BBB disruption. Other subtypes of cells, including $_{S}CTCs$, $_{S}CTECs$, and triploid $_{L}CTCs$, as well as $_{L}CTECs$, did not show a significant correlation with BBB damage.

3.3 | Preoperative small cell-sized triploid CTCs ($_{S}CTCs^{tri}$) correlate with poor prognosis in glioblastoma patients

In general, IDHwt LGG with EGFR amplification, TERT promoter mutation and (or) +7/10− should be diagnosed as GBM.[25] Therefore, in total, 45 molecular GBM patients based on WHO 2021 brain tumor classification were analyzed. All these patients received maximal tumor resection, followed by concurrent chemoradiotherapy and adjuvant temozolomide chemotherapy. In this study, the median PFS (mPFS; Figure 3A) and OS (mOS; Figure 3B) for 45 examined GBM

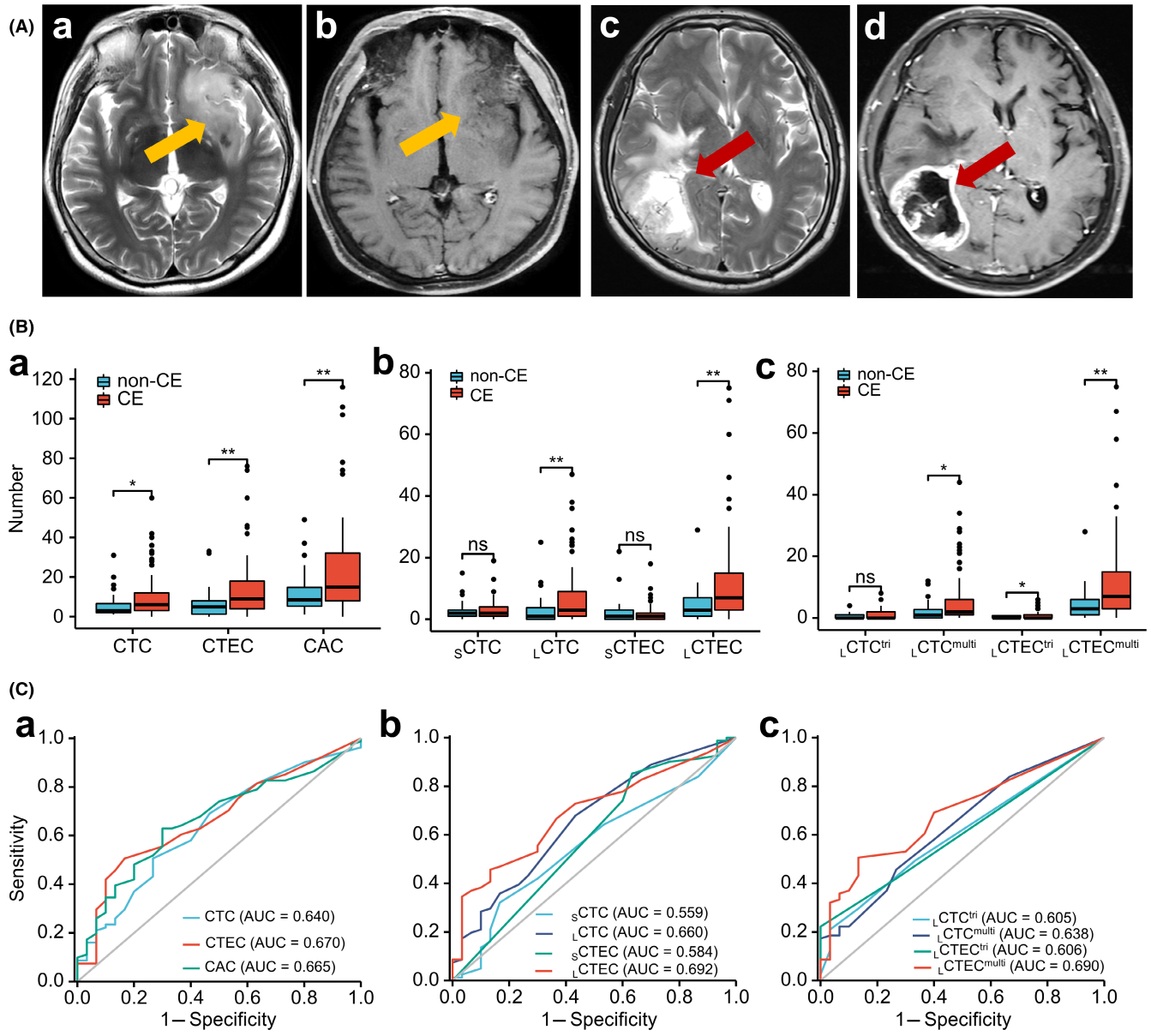

FIGURE 2 Significant increase of large cell-sized multiploid CTECs ($_{L}$CTECs^{multi}) along with contrast-enhancing (CE) lesions. (A) MRI images. (Aa-b): Non-CE lesions (orange arrows). (Ac-d): CE lesions (red arrows). (B) Quantitative analysis of CTCs and CTECs in CE patients ($n = 81$) versus non-CE patients ($n = 30$). (B-a) Overall CTCs and CTECs (median): 6.0 versus 3.0 for CTCs (*$p = 0.023$); 9.0 versus 5.0 for CTECs (**$p = 0.006$); 15.0 versus 8.5 for CACs (**$p = 0.007$). (B-b) Large cell-sized $_{L}$CTCs and $_{L}$CTECs: median 3.0 versus 1.0 for $_{L}$CTCs (**$p = 0.009$); 7.0 versus 3.0 for $_{L}$CTECs (**$p = 0.002$). $_{S}$CTCs and $_{S}$CTECs do not show a significant difference. (B-c) Large multiploid CTCs ($_{L}$CTCs^{multi}) and CTECs ($_{L}$CTECs^{multi}): 2.0 versus 1.0 for $_{L}$CTCs^{multi} (*$p = 0.024$); 7.0 versus 3.0 for $_{L}$CTECs^{multi} (**$p = 0.002$). No significant difference is observed on $_{L}$CTCs^{tri} between non-CE and CE. (C) AUC-ROC curve analysis. (C-a) AUC_{CTEC} (**0.670) > AUC_{CAC} (**0.665) > AUC_{CTC} (*0.640). (C-b) AUC-$_{L}$CTEC (**0.692) > AUC-$_{L}$CTC (**0.660). (C-c) Large multiploid CTEC AUC (**0.690) > large multiploid CTC AUC (*0.638).

patients were 9.3 and 19.0 months, respectively. Compared with the cohort possessing preoperative CTC numbers >11, the cohort having baseline CTCs ≤11 displayed longer mPFS and mOS (mPFS 11.0 versus 3.2 months; **$p = 0.01$; Figure 3Aa; mOS 22.0 versus 12.0 months; **$p = 0.014$; Figure 3Ba). Among those preoperative CTCs, $_{S}$CTCs had a significant impact on early tumor progression (mPFS 13.8 [$_{S}$CTCs ≤2] versus 4.0 months [$_{S}$CTCs >2], **$p = 0.009$, Figure 3Ab; mOS 22.0 [$_{S}$CTCs ≤2] versus 14.0 months [$_{S}$CTCs >2], *$p = 0.03$, Figure 3Bb). Further morphological and karyotypic comprehensive analysis pinpointed that $_{S}$CTC^{tri} was the most sensitive and prominent indicator (mPFS 26.0 [$_{S}$CTCs^{tri} ≤1] versus 5.5 months [$_{S}$CTCs^{tri} >1], *$p = 0.02$, Figure 3Ac; mOS 26.0 [$_{S}$CTCs^{tri} ≤1] versus 14.0 months [$_{S}$CTCs^{tri} >1], *$p = 0.017$, Figure 3Bc). Demonstrated in Figure 3Bd, although patients possessing preoperative CACs ≤28 showed a significantly improved mOS compared with those having CACs >28 (22.0 versus 14.0 months, *$p = 0.041$), CACs were not able

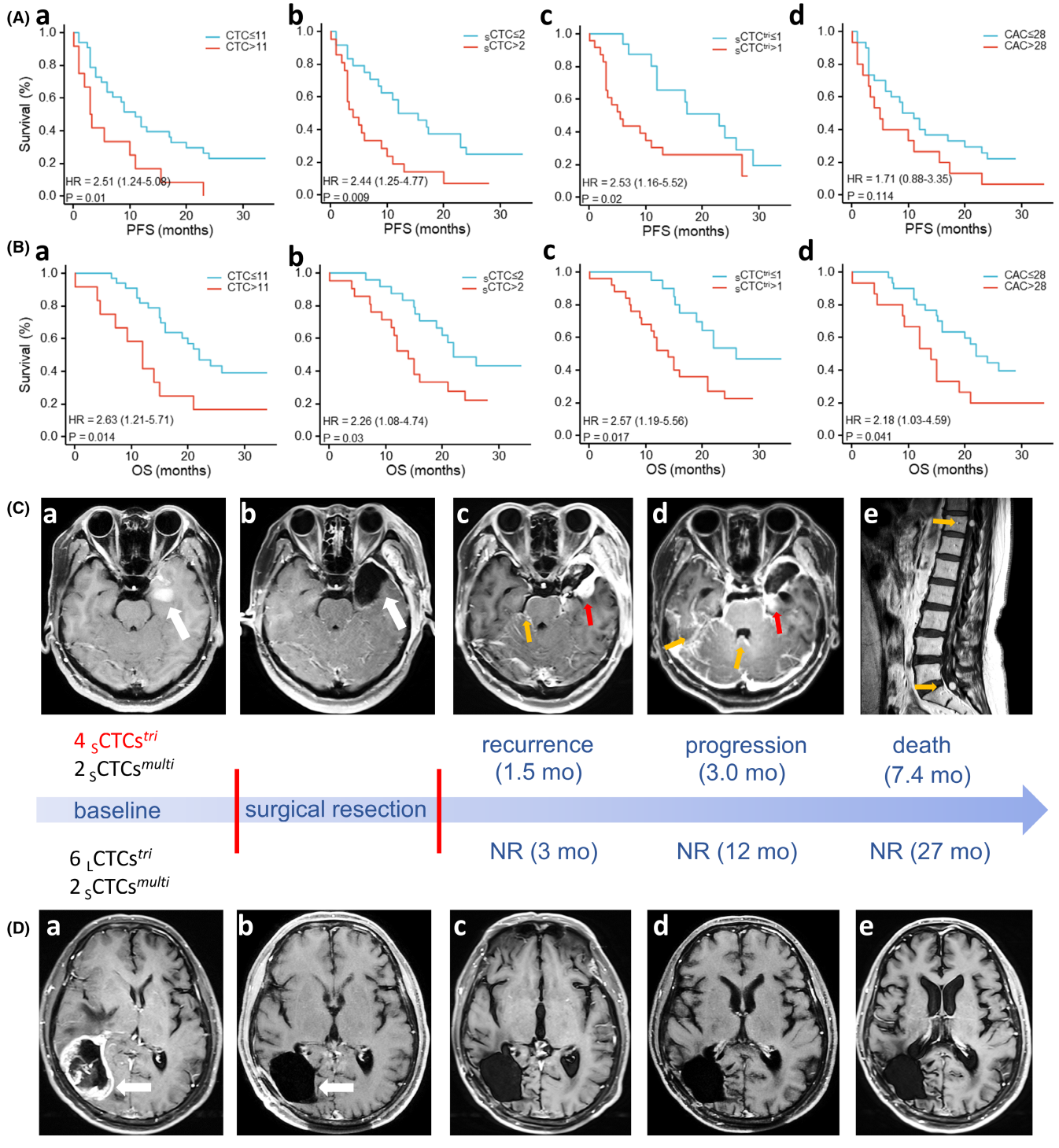

FIGURE 3 Preoperative small cell-sized triploid CTCs ($_{S}CTCs^{tri}$) correlate with poor prognosis in GBM patients ($n = 45$). (A-a) Overall CTCs (cut-off 11), mPFS 11.0 (≤11) versus 3.2 months (>11) (**$p = 0.01$). (A-b) $_{S}CTCs$ (cut-off 2), mPFS 13.8 (≤2) versus 4.0 months (>2) (**$p = 0.009$). (A-c) $_{S}CTCs^{tri}$ (cut-off 1), mPFS 26.0 (≤1) versus 5.5 months (>1) (*$p = 0.02$). (A-d) CACs (cut-off 28), no significant difference is observed ($p = 0.114$). (B-a) CTCs (cut-off 11), mOS 22.0 (≤11) versus 12.0 months (>11) (**$p = 0.014$). (B-b) $_{S}CTCs$ (cut-off 2), mOS 22.0 (≤2) versus 14.0 months (>2) (*$p = 0.03$). (B-c) $_{S}CTCs^{tri}$ (cut-off 1), mOS 26.0 (≤1) versus 14.0 months (>1) (*$p = 0.017$). (B-d) CACs (cut-off 28), mOS 22.0 (≤28) versus 14.0 months (>28) (*$p = 0.041$). (C) $_{S}CTCs^{tri}$ in tumor recurrence and progression. A patient with IDH1/2 wild-type anaplastic astrocytoma (refined as GBM based on the WHO 2021 classification system; C-a, white arrow) had preoperative 4 $_{S}CTCs^{tri}$ and 2 $_{S}CTCs^{multi}$. Tumor was surgically removed (C-b, white arrow). Tumor recurrence (C-c, red arrow) and leptomeningeal dissemination (yellow arrow) were observed 1.5 months after resection, followed by tumor progression in the brain (C-d, red and yellow arrows) and spine (yellow arrows, C-e) until patient's death 7.4 month after surgery (PFS = 1.5 months, OS = 7.4 months). (D) None of $_{S}CTCs^{tri}$ in nonrecurrence patient. A subject with IDH1/2 wild-type glioblastoma (D-a, white arrow) had preoperative 6 $_{L}CTCs^{tri}$ and 2 $_{S}CTCs^{multi}$, but no $_{S}CTCs^{tri}$ was detected. Following surgical removal of the lesion (D-b, white arrow), no recurrence (NR) was observed longer than 27 months (D-c for 3 months, D-d for 12 months and D-e for 27 months).

to effectively evaluate mPFS between those two cohorts of patients (cut-off: 28 CACs, $p = 0.114$, Figure 3Ad), and CTECs did not displayed any prognostic significance (data not shown). Representative cases with high/low burden of $_{S}CTCs^{tri}$ with poor/favorable prognosis are shown in Figures 3C/D.

3.4 | Small cell-sized triploid CTCs ($_{S}CTCs^{tri}$) exhibit resistance to immunoradiotherapy in recurrent malignant glioma patients

A follow-up detection of CTCs and CTECs was performed on 11 recruited patients with recurrent malignant glioma who received subsequent intracranial and systemic immunoadjuvants (poly [I:C]) in combination with low-dose reirradiation (2Gy×3; NCT03392545) (Table 2). Patients were classified into two cohorts of nontreatment responder (progressive diseases/PD, ID 1–5; Table 2), and treatment responder (stable disease [SD, ID 6–7], complete response [CR] or partial response [PR], ID 8–11; Table 2). Exact variation numbers for CTCs (ΔCTCs = PostCTCs − PreCTCs), and CTECs (ΔCTECs = PostCTECs − PreCTECs) in each subject are described in Table 2.

All five subjects (ID 1–5) in the nonresponder cohort showed a substantial increase of CTCs in pace with tumor exacerbation (Figure 4Aa/b, orange), whereas only a slight increase of CTECs in three patients of the same cohort was observed (Figure 4Ac/d, orange). Among the treatment-responder cohort (ID 8–11), a decrease of CTCs in all four patients was revealed following the regression of

TABLE 2 Quantification of CTCs and CTECs in recurrent malignant glioma patients subjected to immunoradiotherapy

ID	Pathology	Treatment	Status	Pre-CTCs	Post-CTCs	ΔCTCs	Pre-CTECs	Post-CTECs	ΔCTECs
1	GBM	C+R	PD	8	176	168	6	36	30
2	O, grade 3	C	PD	11	62	51	13	40	27
3	A, grade 4	C+R	PD	3	34	31	13	15	2
4	GBM	C+R	PD	4	17	13	9	3	−6
5	GBM	C+R	PD	7	16	9	0	17	17
6	GBM	C+R	SD	1	2	1	0	2	2
7	GBM	C+R	SD	5	6	1	0	15	15
8	A, grade 3	C+R	CR	12	8	−4	16	1	−15
9	GBM	S+C+R	CR	8	1	−7	20	0	−20
10	A, grade 3	C+R	CR	30	11	−19	18	6	−12
11	GBM	C+R	PR	93	2	−91	135	0	−135

Abbreviations: A, astrocytoma, IDH mutant and 1p/19q intact; C, chemotherapy; CR, complete remission; GBM, glioblastoma, IDH-wildtype, WHO grade 4; O, oligodendroglioma, IDH mutant and 1p/19q co-deleted; PD, progressive disease; PR, partial remission; R, radiotherapy; S, surgery; SD, stable disease.

FIGURE 4 Small cell-sized triploid CTCs ($_{S}CTC^{stri}$) were resistant to immunoradiotherapy in recurrent malignant gliomas. (A) Variation of CTCs and CTECs in nontreatment responder (PD, orange), and responder (SD/blue, CR/light green or PR/dark green) cohorts. (A-a) ΔCTCs = PostCTCs-PreCTCs. (A-c) ΔCTECs = PostCTECs-PreCTECs. All the PD patients showed a substantial increase in CTCs but only a slight increase in CTECs in three patients of the same cohort. CTCs decreased in all four patients in the treatment-responder cohort (A-b). A similar decrease in CTECs was observed in three out of four patients in the same cohort. Two SD patients did not show a significant change in CTC quantity, but an opposite variation on CTEC amount was revealed (A-d). (B) Prognosis analysis. Compared with CTC quantity increasing cohort (> baseline), CTC decreasing cohort displayed prolonged mPFS (B-a, unreached versus 3.0 months, $^{*}p = 0.047$) and mOS (B-b, unreached versus 14.5 months, $^{*}p = 0.031$). CTECs did not show a significant difference (B-c & B-d). (C) Composition analysis of baseline and post-therapeutic CTCs in responder and nonresponder cohorts. In comparison with the responder cohort (Ca/b), the proportion of pre-therapeutic baseline $_{S}CTCs^{tri}$ in nonresponder cohort (16/33, 48.5%, C-c) was significantly higher than that in the responder cohort (16/142, 11.3%, C-a). Further analysis indicated that following therapy, both $_{L}CTCs^{multi}$ decreased (from 101 to 10) and $_{S}CTCs^{tri}$ (from 16 to 7) in the responder cohort (4Ca/b). In the nonresponder cohort, $_{S}CTCs^{tri}$ and $_{L}CTCs^{multi}$ dramatically increased from baseline 16, 10–36, 228 respectively (Cc/d). This result indicated that a high burden of $_{S}CTC^{tri}$ might lead to therapy resistance and ultimate progression. (D) Dynamic detection of diverse subtypes of CTCs and CTECs along with immunoradiotherapy in a recurrent thalamic glioblastoma patient. Exact numbers of $_{L}CTCs/_{L}CTECs$ (D-a/b, red line), $_{S}CTCs/_{S}CTECs$ (Da/b, aqua line), proportions of different subtypes of CTCs and CTECs detected at each test (D-a/b, bars in different colors), were respectively illustrated in D-a/b/d. MRI images are illustrated in D-c. The patient did not show the visible recurrence (MRI image-a) prior-to therapy at Test 1. Following development of widespread leptomeningeal dissemination at Test 2 (MRI image-b, red arrow), tumor regression at Test 4 (MRI image-c, yellow arrow), and reemergence at Test 5 (MRI image-d, red arrow) along with immunoradiotherapy, quantitative variation of $_{L}CTCs^{multi}$ and $_{L}CTECs^{multi}$ (red lines in D-a and D-b) exactly matched the tumor present status, showing up–down–up path lines. However, the quantity of $_{S}CTCs^{tri}$ (D-a, aqua line) steadily increased, whicj was consistent with ultimate treatment failure.

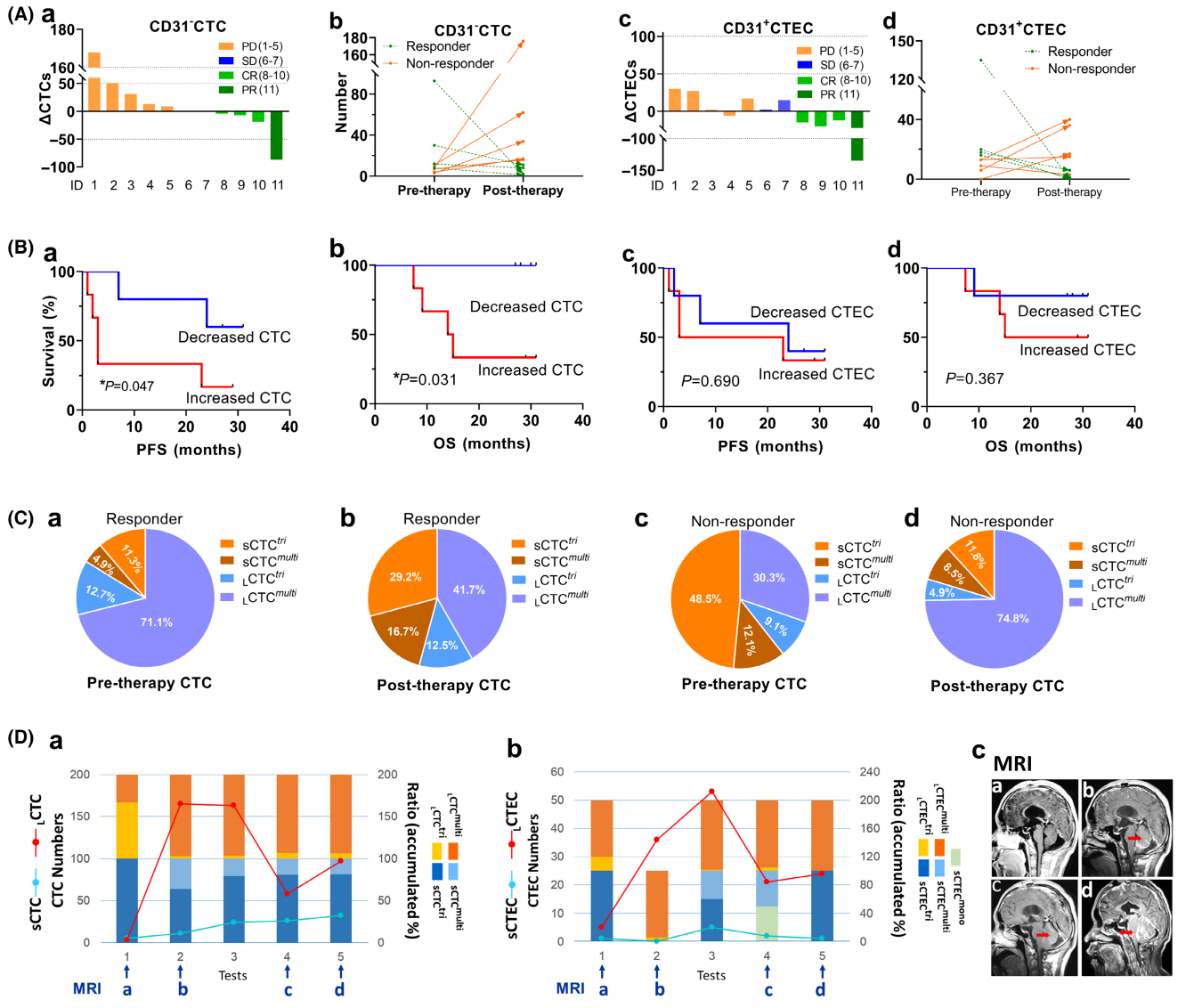

d

		Test 1			Test 2			Test 3			Test 4				Test 5		
		Qty	Tri (%)	Multi (%)	Qty	Tri (%)	Multi (%)	Qty	Tri (%)	Multi (%)	Qty	Mono (%)	Tri (%)	Multi (%)	Qty	Tri (%)	Multi (%)
CTC	small	5	100 (5/5)	0 (0/5)	11	63.6% (7/11)	36 (4/11)	24	79.2 (19/24)	20.8 (5/24)	26	0	80.8 (21/26)	19.2 (5/26)	32	81.3 (26/32)	18.7 (6/32)
	large	3	66.7 (2/3)	33.3 (1/3)	165	3 (5/165)	97 (160/165)	163	3.7 (6/163)	96.3 (157/163)	58	0	6.9 (4/58)	93.1 (54/58)	6.32	6.2 (6/97)	98.8 (91/97)
CTEC	small	1	100 (1/1)	0 (0/1)	0	0	0	5	60 (3/5)	40 (2/5)	2	50 (1/2)	0	50 (1/2)	1	100 (1/1)	0
	large	5	20 (1/5)	80 (4/5)	36	5.6 (2/36)	94.4 (34/36)	53	1.9 (1/53)	98.1 (52/53)	21	0	4.8 (1/21)	95.2 (20/21)	24	0	100 (24/24)

intracranial tumors (green; Figure 4Aa/b, Table 2). A similar decrease in CTECs was observed in three out of four patients in the same cohort (green; Figure 4Ac/d, Table 2). Two SD patients (ID 6 and 7) did not show a significant change in CTC quantity (blue; Figure 4Aa/b, Table 2), but an opposite variation in CTEC amount (blue; Figure 4Ac/d, Table 2). Obtained results suggested that CTC was a more appropriate biomarker in terms of evaluation of therapeutic efficacy in glioma patients.

Prognosis analysis demonstrated that post-therapeutic patients who had a quantity of CTCs less than baseline showed a prolonged mPFS (Figure 4Ba; unreached versus 3.0 mo, $^*p = 0.047$) and a prolonged mOS (Figure 4Bb; unreached versus 14.5 mo, $^*p = 0.031$). However, no statistically significant difference in survival analysis was observed in subjects showing decreased CTECs, revealing $p = 0.690$ for mPFS (Figure 4Bc), and $p = 0.367$ for mOS (Figure 4Bd).

Given that the high burden of $_{S}CTCs^{tri}$ correlated with post-therapeutic patients' inferior outcomes, we further examined the dissected composition of pre-therapeutic and post-therapeutic CTCs in responder and nonresponder cohorts, respectively (Figure 4C). In comparison with the responder cohort (Figures 4Ca/b), the proportion of pre-therapeutic baseline $_{S}CTCs^{tri}$ in the nonresponder cohort (16/33, 48.5%, Figure 4Cc) was significantly higher than that in the responder cohort (16/142, 11.3%; Figure 4Ca). Further analysis indicated that, following therapy, the number of $_{L}CTCs^{multi}$ decreased from 101 to 10 in the responder cohort, and the $_{S}CTCs^{tri}$ significantly decreased from 16 to 7 in the same cohort (Figures 4Ca/b). In the nonresponder cohort, $_{S}CTC^{tri}$ and $_{L}CTCs^{multi}$ dramatically increased from baseline 16, 10–36, 228 respectively (Figure 4Cc/d). This result indicated that the high burden of $_{S}CTC^{tri}$ might lead to therapy resistance and ultimate progression (example in Figure 4D).

4 | DISCUSSION

CTC detection possesses immense potential in terms of therapeutic effect appraisal, potential drug screening, dynamic malignancy surveillance, and prognosis estimation.[26,27] As a novel and advanced technology, there still lacks an integrated strategy to effectively detect and comprehensively characterize CTCs for all types of solid malignancy, particularly for glioma. Extending beyond our previous study showing aneuploid CACs in distinguishing radionecrosis from true tumor progression in patients with different types of gliomas, we applied an SE-iFISH strategy in the current study to further co-investigate how aneuploid $CD31^{-}$ CTCs and $CD31^{+}$ CTECs[17,28] in PB, rather than taking CTCs and CTECs as an entire entity, correlated with BBB disruption, therapeutic resistance, and prognosis in glioma patients. Unlike previously studies which have mainly focused on advanced GBM,[11,12,29] this study recruited patients possessing nearly all diverse types of malignant gliomas at different stages (WHO grades 2–4; Table 1).

The BBB is composed of specialized $CD31^{+}$ BMECs.[6] CD31, the platelet endothelial cell adhesion molecule-1 (PECAM-1) expressed on ECs, can stabilize BBB integrity.[30] A majority of $CD31^{+}$ ECs in the solid tumor vasculature is known as tumor-derived ECs (TECs) exhibiting cytogenetic abnormalities of aneuploid chromosomes.[31] It has been realized that tumor vasculature, contributed by TECs, possesses loosened junctions between ECs, which results in an increase in vascular permeability. In addition, malignant neoplastic cells could hypoxically dedifferentiate into endothelial-like cancer stem cells (CSCs) to form VM channels for reinforced nutrient and oxygen supply.[17,32] Abnormal vasculature, including irregular VM in gliomas, induces disruption and even loss of the BBB.[33] Several intriguing questions, such as whether BMECs bear aneuploid chromosomes, how abnormal ECs (TECs) in circulation (CTECs) correlate with disrupted BBB, and so forth remain to be investigated. Our study suggested that, like visceral tumor TECs, glioma ECs that participated in the constitution of BBB also exhibited aneuploidy. An effective detection of glioma TECs-derived glioma CTECs in PB might help to indicate and evaluate the patient's distorted neovascularization and BBB disruption in real time. In addition, similar to reported circulating glioma cells exhibiting stem cell-like properties with Wnt activation,[29] 14.7% of recruited patients in this study showed $CD133^{+}$ multiploid CTSCs ($_{L}CTSCs^{multi}$) (Figure 1Ae). What those CTSC clinical utilities are and how they relate to the BBB in glioma patients are currently under our investigation.

Aneuploidy has been recognized as the hallmark of malignant neoplastic cells.[16] It has been reported that more than 86% of astrocytomas, GMBs, and gliomas are aneuploid.[34] To investigate how different categories of circulating aneuploid cells impact therapeutic efficacy and prognosis in glioma patients, we examined the clinical relevance of each category of $CD31^{-}$ CTCs, $CD31^{+}$ CTECs and aneuploid CACs. In contrast with conventional cell size or cancer cell surface marker-dependent CTC detection strategies,[35] SE-iFISH enables the performance of in situ co-detection and morphological as well as karyotypic comprehensive characterization of aneuploid CTCs and CTECs, regardless of cell size variation and tumor marker expression.[19,36] Taking advantage of SE-iFISH, we found that a high burden of the specific subtype of $_{S}CTCs^{tri}$ in preoperative subjects might predict postsurgical glioma patients' inferior outcomes (Figure 3), which was in line with a recently published study indicating that presurgical $_{S}CAC^{tri}$ was an effective prognosticator for a poor prognosis in patients with resectable non–small-cell lung cancer (NSCLC).[37] Relevance of triploid CTCs to both breast cancer metastasis[38] and hepatocellular carcinoma (HCC) patient postsurgical recurrence,[39] as well as the correlation between $HER2^{+}$ CTCs with trisomy 8 and gastric patients' prognoses[40] have been reported. Unlike CTCs, presurgical CTECs and their subtypes in this study did not show a significant correlation with postsurgical patient outcome. Moreover, preoperative CACs containing both CTCs and CTECs were also unable to significantly correlate with postoperative patient outcome (Figure 3Ad), suggesting that an effective identification of aneuploid $CD31^{-}$ CTCs and $CD31^{+}$ CTECs was necessary for performing appropriate prognostication of glioma patients.

Further analysis of post-therapeutic CTCs and CTECs in patients subjected to immunoradiotherapy indicated that patients showing a CTC increase following therapy had an inferior mPFS and mOS, and vice versa (Figure 4B). Additional analyses pinpointed that $_{S}CTCs^{tri}$ in responder patients were resistant to therapy, which was in accordance with previously published studies demonstrating that triploid gastric and nasopharyngeal carcinoma CTCs possessed intrinsic resistance to chemotherapy.[41,42] Dynamic monitoring of CTCs and CTECs performed at multiple time intervals along therapy illustrated that the quantity of $_{L}CTCs^{multi}$ and $_{L}CTECs^{multi}$ underwent instant change accompanying tumor present status (Figure 4D), but the variation of $_{S}CTCs^{tri}$ was more consistent with ultimate outcome. Taken together, obtained results suggested that preoperative baseline $_{S}CTCs^{tri}$ might function as a biomarker for prognosticating inferior prognosis, whereas post-therapeutic $_{L}CTCs^{multi}$ and $_{L}CTECs^{multi}$ might be an indicator for timely evaluating therapeutic efficacy in postsurgical glioma patients.

The current study provided a meaningful and practical approach to investigate the clinical significance of glioma CTCs and CTECs.

Additional investigation of several remaining intriguing questions, including how $CD133^+$ CTSCs are relevant to BBB disruption and tumor progression, whether detection of expanded chromosomes beyond Chr8 might enhance detection rate of aneuploid target cells, how positive expression of tumor markers (such as GFAP, EGFR, PTEN) on CTCs and/or CTECs impacted prognosis, the genetic relationship between CTC and primary tumor, and the real association between post-treatment CTC levels and tumor shrinkage or progression, should shed light on further illustrations of the clinical utilities of aneuploid CTCs and CTECs on gliomas.[43]

In conclusion, CACs have widely existed in types of gliomas. The quantity of $CD31^+$ $_L$CTECs^{multi} correlated with CE lesions and BBB disruption. The $CD31^-$ CTCs ($_S$CTCs^{tri}) functioned as an optimal biomarker in prognosticating inferior prognosis. Dynamic surveillance of CTCs reflected the therapeutic response and small CTC might associate with treatment resistance.

AUTHOR CONTRIBUTIONS

Literature search, study design, data interpretation, follow-up, writing: Mingxiao Li, Xiaohui Ren, Shaoping Shen, Haihui Jiang, Chuanwei Yang, Xiaokang Zhang, Xuzhe Zhao, Qinghui Zhu, Ming Li, Yong Cui, Song Lin. Data collection, analysis and interpretation: Faliang Gao, Gehong Dong, Hongyan Chen, Alexander Y. Lin, Daisy Dandan Wang, Mingyang Liu, Peter Ping Lin.

ACKNOWLEDGMENTS

The authors sincerely thank the patients and their families for their participation in the present study. Authors also thank Dr. Lina Zhang (Beijing Tuberculosis and Thoracic Tumor Research Institute, Beijing Chest Hospital, Capital Medical University) and the staff at Cytointelligen (China Medical City, Taizhou, Jiangsu, China) for providing technical assistance.

FUNDING INFORMATION

This study was supported by the Capital's Funds for Health Improvement and Research (2020-2-1075) and the National Natural Science Foundation of China (81771309).

DISCLOSURE

i•FISH® is the registered trademark of Cytelligen. Dr. Peter P. Lin is the president at Cytelligen. None of authors owns Cytelligen's stock shares. No additional conflicts of interest to be disclosed.

ETHICS STATEMENT

The study was approved by the institutional review board of the Capital Medical University.

INFORMED CONSENT

The signed consent forms were received from every patient.

REGISTRY AND THE REGISTRATION OF THE STUDY

N/A.

ANIMAL STUDIES

N/A.

ORCID

Song Lin https://orcid.org/0000-0001-5721-274X

REFERENCES

1. Lapointe S, Perry A, Butowski NA. Primary brain tumours in adults. *Lancet*. 2018;392(10145):432-446. doi:10.1016/S0140−6736(18)30990-5
2. Weller M, van den Bent M, Tonn JC, et al. European Association for Neuro-Oncology (EANO) guideline on the diagnosis and treatment of adult astrocytic and oligodendroglial gliomas. *Lancet Oncol*. 2017;18(6):e315-e329. doi:10.1016/S1470-2045(17)30194-8
3. Mistry AM, Kelly PD, Thompson RC, Chambless LB. Cancer dissemination, hydrocephalus, and survival after cerebral ventricular entry during high-grade glioma surgery: a meta-analysis. *Neurosurgery*. 2018;83(6):1119-1127. doi:10.1093/neuros/nyy202
4. Anghileri E, Castiglione M, Nunziata R, et al. Extraneural metastases in glioblastoma patients: two cases with YKL–40-positive glioblastomas and a meta-analysis of the literature. *Neurosurg Rev*. 2016;39(1):37-45; discussion 45-6. doi:10.1007/s10143-015-0656-9
5. Cai X, Qin JJ, Hao SY, et al. Clinical characteristics associated with the intracranial dissemination of gliomas. *Clin Neurol Neurosurg*. 2018;166:141-146. doi:10.1016/j.clineuro.2018.01.038
6. Qian T, Maguire SE, Canfield SG, et al. Directed differentiation of human pluripotent stem cells to blood-brain barrier endothelial cells. *Sci Adv*. 2017;3(11):e1701679. doi:10.1126/sciadv.1701679
7. Fontanilles M, Duran-Pena A, Idbaih A. Liquid biopsy in primary brain tumors: looking for stardust! *Curr Neurol Neurosci Rep*. 2018;18(3):13. doi:10.1007/s11910-018-0820-z
8. Kros JM, Mustafa DM, Dekker LJ, Sillevis Smitt PA, Luider TM, Zheng PP. Circulating glioma biomarkers. *Neuro Oncol*. 2015;17(3):343-360. doi:10.1093/neuonc/nou207
9. Zachariah MA, Oliveira-Costa JP, Carter BS, Stott SL, Nahed BV. Blood-based biomarkers for the diagnosis and monitoring of gliomas. *Neuro Oncol*. 2018;20(9):1155-1161. doi:10.1093/neuonc/noy074
10. Macarthur KM, Kao GD, Chandrasekaran S, et al. Detection of brain tumor cells in the peripheral blood by a telomerase promoter-based assay. *Cancer Res*. 2014;74(8):2152-2159. doi:10.1158/0008-5472.CAN-13-0813
11. Muller C, Holtschmidt J, Auer M, et al. Hematogenous dissemination of glioblastoma multiforme. *Sci Transl Med*. 2014;6(247):247ra101. doi:10.1126/scitranslmed.3009095
12. Sullivan JP, Nahed BV, Madden MW, et al. Brain tumor cells in circulation are enriched for mesenchymal gene expression. *Cancer Discovery*. 2014;4:1299-1309. doi:10.1158/2159-8290.CD-14-0471
13. Boire A, Brandsma D, Brastianos PK, et al. Liquid biopsy in central nervous system metastases: a RANO review and proposals for clinical applications. *Neuro Oncol*. 2019;21(5):571-584. doi:10.1093/neuonc/noz012
14. Ben-David U, Amon A. Context is everything: aneuploidy in cancer. *Nat Rev Genet*. 2020;21(1):44-62. doi:10.1038/s41576-019-0171-x
15. Chunduri NK, Storchova Z. The diverse consequences of aneuploidy. *Nat Cell Biol*. 2019;21(1):54-62. doi:10.1038/s41556-018-0243-8
16. Gordon DJ, Resio B, Pellman D. Causes and consequences of aneuploidy in cancer. Review. *Nat Rev Genet*. 2012;13(3):189-203. doi:10.1038/nrg3123

17. Lin PP. Aneuploid circulating tumor-derived endothelial cell (CTEC): a novel versatile player in tumor neovascularization and cancer metastasis. *Cell*. 2020;9(6):1539. doi:10.3390/cells9061539
18. Gao F, Cui Y, Jiang H, et al. Circulating tumor cell is a common property of brain glioma and promotes the monitoring system. *Oncotarget*. 2016;7(44):71330-71340. doi:10.18632/oncotarget.11114
19. Lin PP, Gires O, Wang DD, Li L, Wang H. Comprehensive *in situ* co-detection of aneuploid circulating endothelial and tumor cells. *Sci Rep*. 2017;7(1):9789. doi:10.1038/s41598-017-10763-7
20. Ellingson BM, Wen PY, Cloughesy TF. Modified criteria for radiographic response assessment in glioblastoma clinical trials. *Neurotherapeutics*. 2017;14(2):307-320. doi:10.1007/s13311-016-0507-6
21. Wen PY, Macdonald DR, Reardon DA, et al. Updated response assessment criteria for high-grade gliomas: response assessment in neuro-oncology working group. *J Clin Oncol*. 2010;28(11):1963-1972. doi:10.1200/jco.2009.26.3541
22. Li M, Dong G, Zhang W, et al. Combining MGMT promoter pyrosequencing and protein expression to optimize prognosis stratification in glioblastoma. *Cancer Sci*. 2021;112(9):3699-3710. doi:10.1111/cas.15024
23. Li M, Ren X, Jiang H, et al. Supratentorial high-grade astrocytoma with leptomeningeal spread to the fourth ventricle: a lethal dissemination with dismal prognosis. *J Neurooncol*. 2019;142(2):253-261. doi:10.1007/s11060-018-03086-8
24. Li M, Ren X, Chen X, et al. Combining hyperintense FLAIR rim and radiological features in identifying IDH mutant 1p/19q non-codeleted lower-grade glioma. *Eur Radiol*. 2022;32(6):3869-3879. doi:10.1007/s00330-021-08500-w
25. Louis DN, Perry A, Wesseling P, et al. The 2021 WHO classification of tumors of the central nervous system: a summary. *Neuro Oncol*. 2021;23(8):1231-1251. doi:10.1093/neuonc/noab106
26. Heitzer E, Haque IS, Roberts CES, Speicher MR. Current and future perspectives of liquid biopsies in genomics-driven oncology. *Nat Rev Genet*. 2019;20(2):71-88. doi:10.1038/s41576-018-0071-5
27. Keller L, Pantel K. Unravelling tumour heterogeneity by single-cell profiling of circulating tumour cells. *Nat Rev Cancer*. 2019;19(10):553-567. doi:10.1038/s41568-019-0180-2
28. Lin PP, Aneuploid CTC, CEC. Review. *Diagnostics (Basel)*. 2018;8(2):26. doi:10.3390/diagnostics8020026
29. Liu T, Xu H, Huang M, et al. Circulating glioma cells exhibit stem cell-like properties. *Cancer Res*. 2018;78(23):6632-6642. doi:10.1158/0008-5472.CAN-18-0650
30. Wimmer I, Tietz S, Nishihara H, et al. PECAM-1 stabilizes blood-brain barrier integrity and favors paracellular T-cell diapedesis across the blood-brain barrier during neuroinflammation. *Front Immunol*. 2019;10:711. doi:10.3389/fimmu.2019.00711
31. Hida K, Klagsbrun M. A new perspective on tumor endothelial cells: unexpected chromosome and centrosome abnormalities. *Cancer Res*. 2005;65(7):2507-2510. doi:10.1158/0008-5472.CAN-05-0002
32. Friedmann-Morvinski D, Verma IM. Dedifferentiation and reprogramming: origins of cancer stem cells. *EMBO Rep*. 2014;15(3):244-253. doi:10.1002/embr.201338254
33. Delgado-Bellido D, Serrano-Saenz S, Fernandez-Cortes M, Oliver FJ. Vasculogenic mimicry signaling revisited: focus on non-vascular VE-cadherin. *Mol Cancer*. 2017;16(1):65. doi:10.1186/s12943-017-0631-x
34. Duijf PH, Schultz N, Benezra R. Cancer cells preferentially lose small chromosomes. *Int J Cancer*. 2013;132(10):2316-2326. doi:10.1002/ijc.27924
35. Yu M, Stott S, Toner M, Maheswaran S, Haber DA. Circulating tumor cells: approaches to isolation and characterization. *J Cell Biol*. 2011;192(3):373-382. doi:10.1083/jcb.201010021
36. Lin PP. Integrated EpCAM-independent subtraction enrichment and iFISH strategies to detect and classify disseminated and circulating tumors cells. *Clin Transl Med*. 2015;4(1):38. doi:10.1186/s40169-015-0081-2
37. Hong Y, Si J, Zhang J, et al. Small cell size circulating Aneuploid cells as a biomarker of prognosis in Resectable non-small cell lung cancer. *Front Oncol*. 2021;11:590952.
38. Liu X, Li J, Cadilha BL, et al. Epithelial-type systemic breast carcinoma cells with a restricted mesenchymal transition are a major source of metastasis. *Sci Adv*. 2019;5(6):eaav4275. doi:10.1126/sciadv.aav4275
39. Wang L, Li Y, Xu J, et al. Quantified postsurgical small cell size CTCs and EpCAM(+) circulating tumor stem cells with cytogenetic abnormalities in hepatocellular carcinoma patients determine cancer relapse. *Cancer Lett*. 2018;412:99-107. doi:10.1016/j.canlet.2017.10.004
40. Li Y, Zhang X, Liu D, et al. Evolutionary expression of HER2 conferred by chromosome aneuploidy on circulating gastric cancer cells contributes to developing targeted and chemotherapeutic resistance. *Clin Cancer Res*. 2018;24(21):5261-5271. doi:10.1158/1078-0432.CCR-18-1205
41. Li YL, Zhang XT, Ge S, et al. Clinical significance of phenotyping and karyotyping of circulating tumor cells in patients with advanced gastric cancer. *Oncotarget*. 2014;5(16):6594-6602.
42. Zhang J, Shi H, Jiang T, Liu Z, Lin PP, Chen N. Circulating tumor cells with karyotyping as a novel biomarker for diagnosis and treatment of nasopharyngeal carcinoma. *BMC Cancer*. 2018;18(1):1133. doi:10.1186/s12885-018-5034-x
43. DeWeerdt S. The genomics of brain cancer. *Nature*. 2018;561(7724):S54-S55. doi:10.1038/d41586-018-06711-8

How to cite this article: Li M, Gao F, Ren X, et al. Nonhematogenic circulating aneuploid cells confer inferior prognosis and therapeutic resistance in gliomas. *Cancer Sci*. 2022;113:3535-3546. doi: 10.1111/cas.15516